Light-assisted adsorption of methylene blue dye onto *Luffa cylindrica*

Akanimo Emene[a], Uduak G. Akpan[b,*], Robert Edyvean[a]

[a]*Department of Chemical and Biological Engineering, University of Sheffield, Western Bank, Sheffield, S10 2TN, United Kingdom, emails: ask4akmx@gmail.com (A. Emene), r.edyvean@sheffield.ac.uk (R. Edyvean)*
[b]*Department of Chemical Engineering, Federal University of Technology, Minna, Niger State, Nigeria, email: ugaekon@yahoo.co.uk*

ABSTRACT

This paper reports an investigation into the adsorption of methylene blue (MB – as representative of a group of potentially polluting chemicals) by modified *Luffa cylindrica* (LC). A simple and efficient preparation was employed to treat LC which then successfully and rapidly adsorbed methylene blue in the presence of light. The combination of photodegradation and adsorption of MB occurred simultaneously. The effects of contact time, solution pH, temperature, and initial adsorbate concentration are described. The LC was characterized by Brunauer–Emmett–Teller, Fourier transform infra-red, and scanning electron microscopy with energy-dispersive X-ray analyses. The treated LC adsorbed methylene blue dye from aqueous solution within 5 min at an optimum pH of 7. The experimental data best fitted the Freundlich model, with R^2 = 0.998 and a maximum adsorption capacity of 98.5% at pH 7. There is a difference in adsorption capacity in dark and light conditions. The kinetic data was represented by the pseudo-second-order (PSO) model. This study shows the potential of chemically modified LC to treat wastewater contaminated by methylene blue dye and similar chemicals.

Keywords: Adsorption; Methylene blue; *Luffa cylindrica* (LC); Alkali treated *Luffa cylindrica* (ATLC); HCl treated *Luffa cylindrica* (HTLC)

1. Introduction

Clean water is a valuable asset but achieving this is an ever greater challenge due to increasing pollution. Wastewater from the textile, printing, paper, leather, metal plating, and food processing industries contain pollutants, mainly dye. The toxicity of these pollutants poses an environmental hazard to man and the ecosystem [1]. Dyes, due to their complex aromatic structures, hydrophilic nature, high stability against temperature, water, chemicals, and light, are not easily degraded by conventional water treatment processes [2].

Methylene blue (MB) is a common substance frequently used to dye materials and can be used as a convenient model of a group of potentially polluting chemicals. It is used in various applications such as in the medical field including antimicrobial chemotherapy, cell staining, and cancer research [3]. MB can be freely photo-sensitized by white light to produce very reactive oxygen species. Methods utilized to treat wastewater containing dyes include oxidation processes, ultrafiltration, chemical precipitation, photocatalytic degradation, nanofiltration, biological treatment, adsorption onto various types of carbon, and use of nanomaterials [1,4–6]. The disadvantages of using these methods include high cost, large production of sludge, membrane fouling, and regeneration which increases power consumption and low biodegradability, hence there is a need to develop an efficient treatment method that uses low-cost materials [4].

Adsorption, a highly efficient, cost-effective, and environmental friendly method, has been considered for dye

* Corresponding author.

removal [1]. The United States Environmental Protection Agency (USEPA) has classified adsorption as a top control method for wastewater treatment [3]. In the adsorption process, adsorbents that effectively remove large quantities of pollutants when used in small amounts are preferred. The advantages of liquid-phase adsorption are its low cost, energy efficiency, absence of sludge formation, and simplicity of design and operation. Adsorption materials are commonly prepared by pretreating with various organic solvents and acid/basic solutions [3]. To determine adsorption performance, the kinetics and the quantity of dye retained on the adsorbent are the two most important indices of the adsorption system.

Various biomaterials have been used as efficient adsorbents for the removal of methylene blue and other dyes. Amongst the range of adsorbents, various biomaterials, such as lignin and chitosan have been investigated for the removal of dyes [4,7–9]. Lignin and chitosan have been reported to remove dyes from aqueous solutions. Lignin obtained from plants is considered a low-cost by-product. Biosorbents have a high potential for pollutant removal and remediation due to their high surface area and selective adsorption behavior toward cations giving a high adsorption capacity, and loofa could be regarded as a good adsorbent [2]. The adoption of adsorption processes using loofa will help to curb environmental issues related to aqueous pollutants and their removal [10–13].

This study focuses on the fibrous dried fruit body of the loofa plant, *Luffa cylindrica* (LC), one of a number of species of loofa. Loofa becomes very fibrous when the fruit is fully ripened. Various dishes of gilki, which are made from loofa, are prepared and eaten in India. The fully developed fruit is the source of the loofa scrubbing sponge, which is used in bathrooms and kitchens. The LC was modified in both acid and basic solutions and then used to remove methylene blue from the aqueous solution. These conditions included light and dark to study the co-effect of photodegradation with the adsorption process, contact time, initial pH, and dye concentration. The kinetics were calculated to establish the efficiency of adsorption with the aim of developing an effective specific water treatment process [3].

2. Experimental

2.1. Reagents and stock solutions

All chemicals utilized were of analytical grade. The stock solution, 1 g/L of methylene blue was prepared by dissolving methylene blue dye powder (Sigma-Aldrich, United Kingdom) in deionized water. The desired concentrations were obtained by diluting the stock solution to set concentrations, varying from 5 to 40 mg/L. Solutions of 0.1 M HCl and 0.1 M NaOH were used to adjust the solution pH.

2.2. Chemical modification of L. cylindrica

Dried fruit of LC were purchased in the United Kingdom. The pale yellow *L. cylindrica* fiber was washed several times with distilled water to remove surface impurities and seeds, then alkali treated LC (ATLC) by soaking in 4% NaOH at room temperature for 1 h. The same procedure

was used with 4% HCl to obtain HCl treated *L. cylindrica* (HTLC). The material was repeatedly washed in distilled water until the pH was neutral, and then oven-dried at 90°C for 24 h. The dried samples were grinded and sieved to 1 mm particle size and stored for utilization in experiments.

2.3. Characterization of LC

2.3.1. Surface analysis of ATLC, HTLC, and LC

The surface structure of LC was analyzed by an analytical scanning electron microscopy (Model JOEL JSM-6010LA) coupled with energy-dispersive X-ray (EDX) with an accelerating voltage of 10 kV at a magnification of ×550 SS60. Chemical characteristics were determined using a Nicolet 6700 Fourier transform infra-red (FT-IR) spectrometer (USA) to identify the functionality that interacts with MB ions. 50 mg of dried LC and treated LC (<250 μm thickness) were prepared for attenuated total reflectance with Fourier transform infra-red (ATR-FTIR) analysis. Measurements were made in transmittance mode using a spectral resolution of 4 cm^{-1} by 256 scans and approximately 150 s per step across the range 4,000 to 650 cm^{-1}. The surface area of each sample of LC was determined from nitrogen adsorption at 77.2 K in the range of relative pressure (p/p^0) of 0.05–1 by using a Micromeritics 3Flex instrument (United Kingdom). The samples were degassed at 150°C for 24 h. A three-parameter non-linear fitting procedure was used and the LC samples were subjected to a 99-point Brunauer–Emmett–Teller (BET) surface analysis and full adsorption isotherms were collected for all samples. The conventional single point method of relative pressure was used.

2.3.2. Point of zero charge determination

50 mL of 0.01 M NaCl solution was introduced into 250 mL Erlenmeyer flasks and 0.5 g of LC was added to each of them. The pH value of each solution was adjusted in the range of 2–12 by the addition of 0.1 M HCl or NaOH solutions. Each flask was agitated for 48 h and the final solution pH measured by a pH meter. The final pH was plotted against the initial pH. The point of intersection of the curve was taken as the pHpzc [14].

2.3.3. Light intensity measurements

Batch adsorption studies were carried out under different visible light intensities, 0.17 and 820 lux. Experiments were carried out at a concentration of 10 mg/L at pH 7. The treated LC (ATLC) and methylene blue were continuously mixed for a period of 90 min at room temperature (21°C) on a magnetic stirrer. The absorbance of the residual dye solutions was analyzed using a spectrophotometer (Spectronic TM 200E Thermo Scientific Version 4.04i, United Kingdom).

2.4. Batch extraction experiments

All batch extractions as a function of acid concentration were carried out as single contacts with the contact of 1 g of each treated *L. cylindrica* (ATLC, HTLC, and LC) with 100 mL of dye solution at MB concentrations of 5, 10, 15, 20, 30, and 40 mg/L. To determine the effect of pH a set of experiments

was carried out at pH 4, 5, 6, 7, and 8 at an MB concentration of 10 mg/L. To determine the effect of temperature, ATLC and dye solution were continuously mixed for a period of 24 h at temperatures of 21°C, 35°C, 45°C, and 55°C. Distribution behavior was determined using the following:

$$D_W = \left(\frac{C_i - C_{aq}}{C_{aq}} \right) \times \frac{V_{aq}}{m_{Luffa}} \tag{1}$$

where D_W is the weighted distribution of the analyte where C_i is the initial aqueous activity of the analyte before contact and C_{aq} is the aqueous activity of the analyte after equilibration. V_{aq} is the volume of the aqueous phase (mL) and m_{Luffa} is the mass of the LC and treated LC (g). The extraction percentage was determined by difference (Eq. (2)) and the concentrations of the MB determined using a spectrophotometer:

$$E\% = \frac{C_i - C_{aq}}{C_i} \times 100 \tag{2}$$

where C_i is the initial MB concentration before contact and C_{aq} is the concentration of the MB in the aqueous phase after contact with the LC and treated LC. Error was determined by triplicate measurements.

2.5. Determination of loading behavior

All loading isotherms were carried out as single contacts using 1 g of ATLC, HTLC, and LC with 100 mL of dye solution. The adsorbent and dye solution were continuously mixed for 24 h at room temperature (21°C). A widely researched and commonly used two-parameter fitting model was used to determine the fitting ability due to its quantitative criteria for evaluation [15,16]. The 3-parameter model which gives a clearer evaluation of the data was also utilized. The data were fitted to Langmuir, Dubinin–Radushkevic [17], Temkin, and Sips models, Eqs. (3)–(10). The fitting was carried out by using linear regression and by non-linear least-squares analysis using SOLVER [18].

Langmuir:

$$q_e = \frac{K_L C}{1 + a_L C} \tag{3}$$

where q_e is the adsorption capacity, C is the concentration at equilibrium and a_L and K_L are constants. The monolayer saturation capacity, q_m (g/L$_{wsr}$), was calculated from the Langmuir equation using Eq. (4).

$$K_L = q_m a_L \tag{4}$$

Dubinin–Radushkevich:

$$q_e = q_D \exp \left(-B_D \left[RT \ln \left(1 + \frac{1}{C} \right) \right]^2 \right) \tag{5}$$

where q_D is a constant in the Dubinin–Radushkevich model which is related to adsorption capacity and B_D is a

constant which relates to the mean free energy of adsorption; R (J/mol K) is the gas constant; and T (K) is the absolute temperature.

Where the mean free energy of sorption, E, can be calculated using B_D in Eq. (6):

$$E = \frac{1}{\sqrt{2B_D}} \tag{6}$$

Sips:

$$q_e = \frac{K_s C_e^{\beta_s}}{1 + K_s C_e^{\beta_s}} \tag{7}$$

where K_s (dm^3/mmol) is associated with energy of adsorption and β_s indicates the system heterogeneity (3).

Temkin:

$$q_e = B \ln A + B \ln C_e \tag{8}$$

$$B = \frac{RT}{b_t} \tag{9}$$

where R is the universal gas constant, T is the absolute temperature (K), b_t is heat of adsorption, and A is equilibrium binding constant. A plot of q_e vs. $\ln C_e$ enables the determination of constant b_t and A.

Error in the isotherm constants was calculated from the linearized form of the model using the SOLVER calculated values using the deviations of the experimental data from the best-fit line.

2.6. Determination of the kinetics of extraction

Batch kinetics were determined by contacting 0.5 g adsorbent with 100 mL of dye solution, continuously mixed for a period of 24 h at 21°C. 5 mL of samples were extracted at preset time intervals. The pseudo-first-order was not used to fit the data because this model does not show the involvement of two species, which best describes the adsorption process. The data were fitted using a linear fit of pseudo-second-order models which do not take into account the mechanism of reaction.

The linear form of the pseudo-second-order kinetic model [19] is given in Eq. (10):

$$\frac{t}{q_t} = \frac{1}{kq_e^2} + \frac{1}{q_e} t \tag{10}$$

where k is the pseudo-second-order reaction constant (h^{-1}). Eq. (11) is the non-linear form for the pseudo-second-order kinetics:

$$q_t = \frac{kq_e^2 t}{1 + kq_e t} \tag{11}$$

The non-linear form was fitted using the minimization of the sum of square errors (SSE) using SOLVER [19].

3. Results and discussion

3.1. Chemical modification of LC

The LC morphology as shown in Fig. 1a appears dry and flaky with many loose particles on the surface. In Fig. 1b, the morphology of the NaOH treated LC (ATLC) is more broken up with few loose particles on the surface. This may result in the exposure of the pores for further adsorption [20]. In Fig. 1c, the morphology of methylene blue loaded ATLC shows a smooth surface which indicates adsorption into the pores of the LC. FTIR (Fig. 2) was used to determine the nature of the functional groups present on the LC, ATLC, and HTLC surface. Treating LC fibers with 4% NaOH leads to a higher crystallinity index and to an improvement in adhesion capacity [20,21]. It has
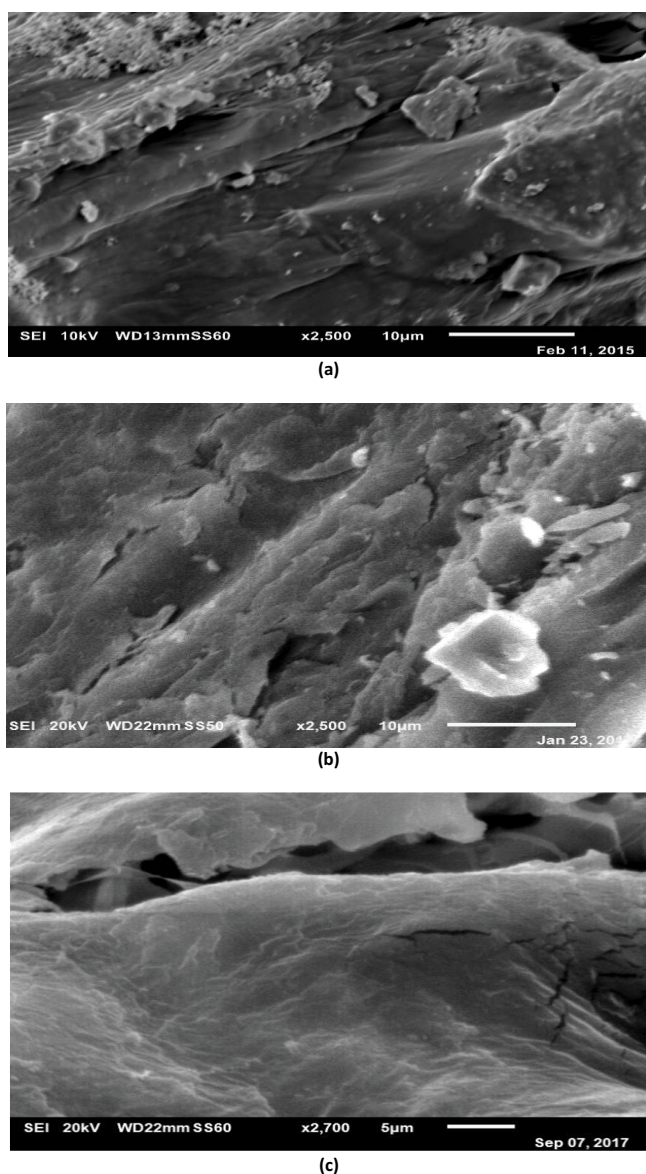
also been reported that HCl chemical treatment greatly enhances the adsorption capacity of adsorbents [22].

Treatment with acids and alkalis has been widely used to enhance the sorption properties of biomaterials [21]. Alkali treatment has been used to enhance the properties of loofa [21] and the maximum percentage of NaOH to treat loofa without damage to the crystalline region is reported to be 8% [23]. Modification of loofa with 4% NaOH bestows additional functionality of OH⁻ groups onto its surface [24]. Modification of loofa with 4% HCl gives an increased surface area as compared to untreated loofa (Fig. 1b). The higher the pKa (deprotonation constant) the greater the adsorption preference on the ATLC surface [25]. Table 1 presents the BET results for the modified and unmodified LC.

The BET surface area of NaOH treated loofa (43.10 m^2/g) is higher than untreated loofa (25.32 m^2/g. BET surface area of HCl treated loofa is 2.14 m^2/g higher than the untreated loofa. This shows an increased surface area which accounts for the broken up and rougher loofa surface. The increase in surface area after alkali and acid treatment by 70.22% and 8.49%, respectively, and the resulting increase in adsorption indicates the involvement of the loofa surface and pores in enhancing the adsorption process.

The FT-IR spectra of LC, ATLC, and HTLC loaded with MB are shown in Fig. 2.

The change in the adsorption bands between untreated and treated loofa indicate characteristic functional groups on the adsorbent and a change in the bands across the range 800–4,000 cm^{-1}, and also a change in the surface chemistry of the alkali and acid-treated loofa is observed at various points as shown in Table 2.

The peak at 3,330 cm^{-1} is attributed to bonded groups of the O–H group. The bands observed at 2,300 cm^{-1} are assigned to C≡N group and the shift in the bond at 2,800 cm^{-1} is attributed to the aliphatic C–H group in the methyl group. A shift in peak intensity (Fig. 2) indicates a change in the binding energy pattern [23,25,28,29]. This indicates the involvement of O–H, C–H, and C–O bonds (wavenumber range of 1,000–3,300 cm^{-1}) in the adsorption of MB onto loofa. A similar change in peak intensity occurs with the untreated, NaOH and HCl treated loofa. The new peaks formed at 1,610 and 1,235 cm^{-1} after the adsorption of MB onto untreated loofa can be attributed to the stretching of the carbonyl groups and bending vibrations of the C–H of the methyl group [30]. For the HCl treated MB loaded
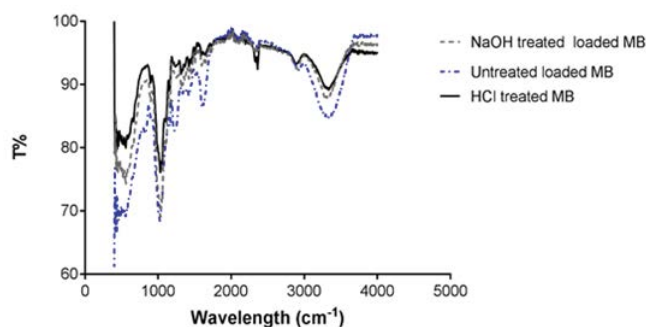

Fig. 1. Electron microscope surface morphology of loofa. Structural morphology of (a) raw loofa (untreated), (b) 4% NaOH treated loofa, and (c) MB loaded 4% NaOH treated loofa.

Fig. 2. FT-IR spectra of ATLC, HTLC, and untreated loofa loaded with MB at 21°C (256 scans).

Table 1
BET results for modified and unmodified LC

Data	Untreated	NaOH treated	HCl treated
Surface area (m²/g)	25.32	43.10	27.47
Specific surface area (m²)	5.75	7.00	6.45
Total pore volume (cm³/g)	0.01	0.02	0.01

Table 2
Change in transmission FTIR results at specific regions of absorbance

Region	$\Delta T\%$	Corresponding absorbance	Reference
1,265–1,460 cm⁻¹ (fingerprint region)	+0.6 to +1.1	O–H bending	[11,12]
1,540 cm⁻¹	−0.85	N–H bending	[13]
1,735 cm⁻¹	+0.6	C=O stretching (carbonyl group of ketone)	[11]
2,890 cm⁻¹	+0.8	C–H stretching	[25,26]
3,340 cm⁻¹	+1.6	O–H bonding	[11,25,27]

loofa, the band shift is also in the wavelength range of 1,000–3,300 cm⁻¹. The FT-IR vibrations of all the loofa used are altered and both NaOH and HCl treated loofa loaded with MB show a significant change at 3,300 cm⁻¹ which indicates a strong bond of the carboxylic group as the dominant group in adsorption leading to a higher adsorption capacity as compared to untreated loofa loaded with MB.

The peak shift from 3,300 to 3,322 cm⁻¹ indicates that an adsorption has occurred, and in this case, the adsorbed species is OH⁻ (additional OH⁻ group). On the other hand, NaOH treatment disrupts the hydrogen bonding of OH⁻ functional groups, ripping off H⁺ and allowing adsorption to occur [31,32]. Carboxyl groups are the dominant functional groups of ATLC in adsorption. Therefore, the difference in the binding energy of the functional groups as shown by the spectra peaks indicates the important role of O–H in the adsorption of MB ions onto ATLC [33]. The characteristic bands on the loofa surface show the structure of the loofa to include lignin, cellulose, and hemicellulose.

3.2. Adsorption studies onto ATLC as a function of acid and anion concentration

The effect of time on the extraction of MB onto LC and ATLC are shown in Fig. 3. There is an enhancement in the removal capacity of loofa after treatment when compared to LC.

3.3. pH effect

pH is the most important controlling factor in the adsorption process of cations [34]. At equilibrium pH lower than 5 the lower adsorption is attributed to the competition of H⁺ for the binding sites on ATLC thereby reducing the adsorption capacity. At pH above 6, the decrease in MB uptake is most likely due to the hydrolysis of the MB ion in solution. This shows the difference in MB species and their ability to be adsorbed at different solution pH. Furthermore, optimum adsorption of MB ions occurs below
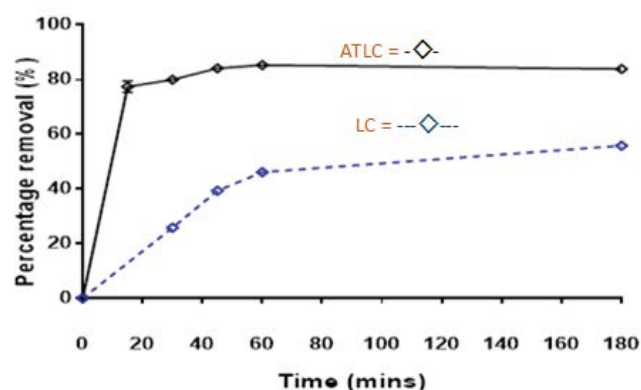

Fig. 3. Effect of time on the percentage extraction of MB after 3 h contact; 50 mg/L MB initial concentration; agitation at 200 rpm; at a temperature of 21°C, 5 g/L biosorbent dosage (LC = ---◇--, ATLC = -◇-).

the point of zero charges, which is concentrated at the interface. The pH$_{pzc}$ was determined to be at 7.2 for LC (Fig. 4). Since, at a pH$_{pzc}$ of 7.2, the ionic charge is positive at a lower pH and negative at a higher pH, the electrostatic attraction is opposed as the maximum uptake occurs between pH 5 and 7. Therefore, the adsorption process is dominated by ionic exchange and other adsorption mechanisms [34–38]. The effect of pH is shown in Fig. 5. It can be seen that the percentage extraction passes through a maximum between pH 6 and 8. A closer observation of Fig. 5 reveals that the adsorption of MB between acidic pH 4 and 6 has an irregular pattern for both modified LC which may be as a result of how the loofa binds differently as compared to untreated LC which shows a steady increase in MB adsorption as pH increases. This is explained by an uneven distribution of MB cations on the surface and pores of the loofa. The difference in percentage removal between the varying pH 5 and 6 is −3. As the rate constant (K – pseudo-second-order) of MB adsorption increases, the amount of OH⁻ in solution is
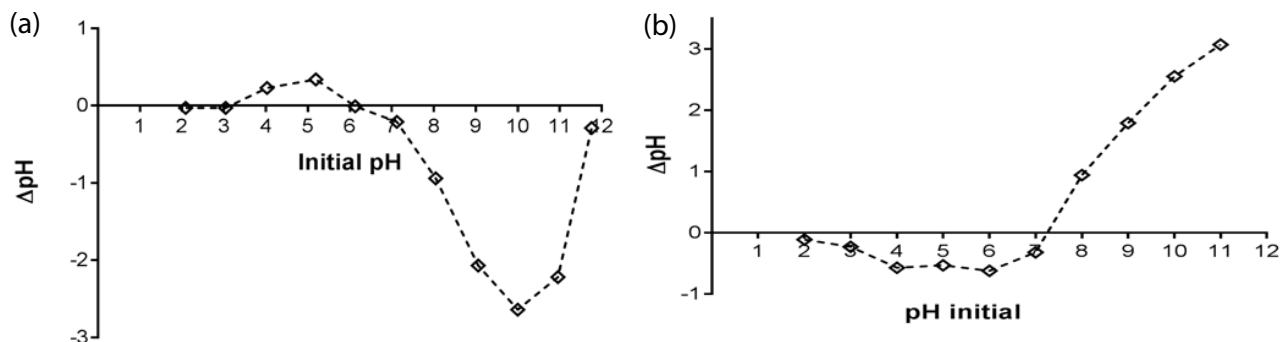
Fig. 4. Point of zero charges (pHpzc) determination for the (a) untreated loofa and (b) alkali-treated loofa.
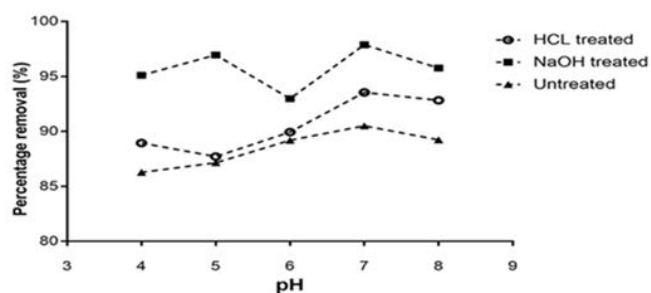

Fig. 5. Effect of solution pH conditions on the percentage extraction of MB after 60 min contact; MB ion concentration: 50 mg/L; agitation at 200 rpm; at temperature 21°C and 5 g/L biosorbent dosage.
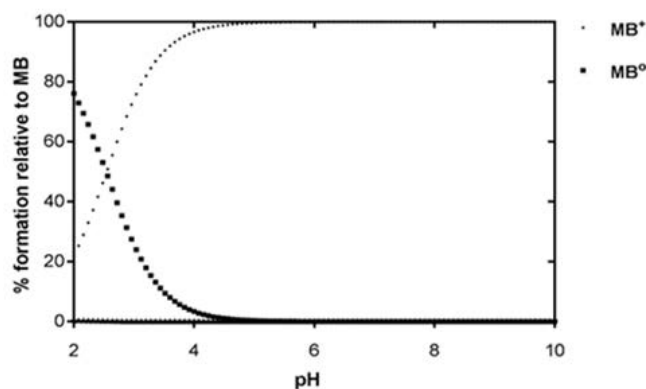

Fig. 6. Distribution of MB species in aqueous solution as a function of pH.

increased leading to an increase in pH. The rate of adsorption increases as pH increases over time.

The potential effect of MB ion speciation as a function of pH is presented in Fig. 6 as carried out using the Hyss2009 program and stability constants from the NIST database. The solution pH has a prominent effect on MB speciation in solution. MB exists as a cationic species (MB^+) and undissociated molecules (MB^0) in an aqueous solution [26]. Different aggregation forms of MB occur when MB is dissolved in aqueous solutions. Using the equilibrium aggregation constants, an attempt was made to determine the speciation of MB in water solution as the pH changes. As shown in Fig. 6, at a pH = 3, the MB cationic species and the undissociated MB molecules coexist. As the pH increases, the undissociated MB molecule decreases and the cationic species increases until it is the only available MB form [26]. As the pH increases over pH 6, the cationic species of MB is 100% and therefore dominates the adsorption process. The MB free ions (cationic species) are the dominant species on the loofa in an alkaline medium [26].

Fig. 7 shows the effect of temperature on MB extraction from an aqueous solution. It is clear from the figure that as temperature increases from 21°C to 55°C, the percentage removal of MB is decreased by approximately 3% at equilibrium (60 min). This indicates that the adsorption on alkali-treated loofa is not favored by an increase in temperature (Fig. 7). This confirms that the binding of the MB adsorbed to the alkali-treated LC decreases with the increase in temperature.
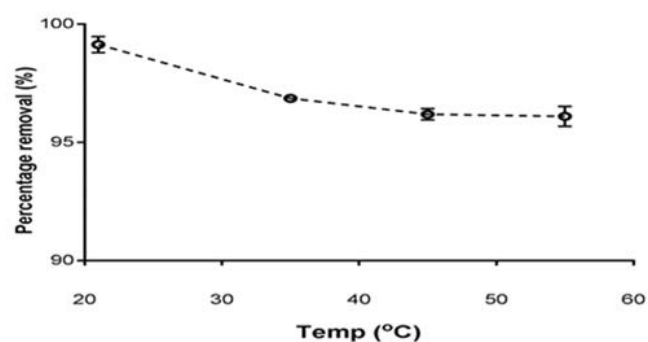

Fig. 7. Effect of temperature on MB extraction from aqueous solution at pH 7; MB concentration 10 mg/L; agitation speed: 200 rpm; temperature range: 21°C–55°C, 1 h contact time, 5 g/L alkali-treated loofa dosage. Data from three replicate measurements.

3.4. Isotherm behavior of adsorption

The isotherm fitting parameters for all the isotherm models tested on ATLC are given in Table 3 based on linear regression and non-linear regression using SOLVER [26,39]. The isotherms are used to determine the best-fit in order to explain and suggest the model that best predicts the biosorption that occurs [40].

Table 3
Parameters obtained for various isotherm models for MB adsorption onto ATLC using non-linear and linear least-squares fitting using SOLVER

Freudlich		Sips	
Constant	Value	Constant	Value
K_F	8.9 ± 0.2	K_S	2.8 ± 0.01
n_F	1.9 ± 0.5	n	0.5 ± 0.02
		q_m (mg/g)	4.2 ± 0.05
R^2	0.998	R^2	0.689
Dubinin–Radushkevich		Temkin	
Constant	Value	Constant	Value
B_D (×10^{-9})	2.0 ± 0.2	K_T	10.3 ± 0.05
q_D (mol/g) (×10^{-4})	3.8 ± 0.2	b_T (×10^8)	2.0 ± 0.5
E_D (kJ/mol)	15.8 ± 0.7	R^2	0.671
R^2	0.667		

Experimental conditions: the temperature at 21°C, 24 h contact time, 20 mg/L initial concentration, and pH 7.

The relationship between the equilibrium concentration and adsorption capacity (a gradual increase in uptake capacity) is shown in Fig. 8. The Temkin, Freudlich, Sips, and Dubinin–Radushkevich were the isotherm models used to fit the experimental data because Langmuir model was not sufficient to explain the adsorption behavior of the methylene blue uptake. The adsorption behavior of MB ions is best fitted by the Freudlich model (Fig. 8) with a R^2 value of 0.998. This indicates multilayer adsorption.

In column testing, MB adsorption equilibrium was found to occur faster for LC (30 min) compared to ATLC (60 min). This indicates a longer breakthrough time for the modified LC.

The model fitting of MB ion biosorption behavior of LC indicates a heterogeneous surface. The Freudlich isotherm model shows the best fit which suggests a heterogeneous distribution of adsorption sites [41]. The value of 1/n at 0.52 measures the surface heterogeneity, which becomes more heterogeneous with a value closer to 1 [17]. The K_L values at 8.9 L/mg relate to higher binding energy of adsorption which leads to higher adsorption capacity [27,41]. Modification of the loofa with 4% HCl and 4% NaOH improves the adsorption capacity of MB by 3.6% and 6.5%, respectively. Compared to other treated loofa adsorbents (Table 4), NaOH modified loofa (ATLC)
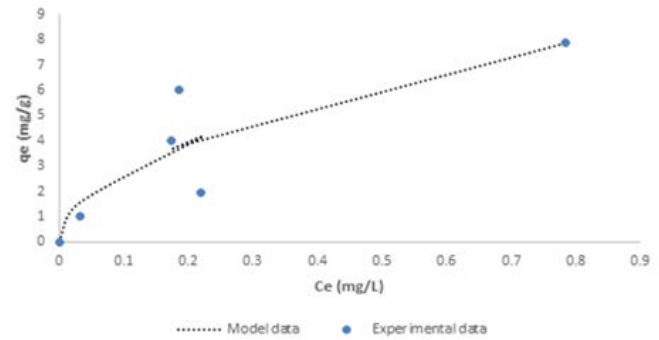

Fig. 8. MB isotherm at pH 7 ± 0.1, 21°C, and 24 h. contact time. Freundlich model fit is shown by the dashed line.

shows the highest percentage removal of MB over a short period of time at room temperature.

3.5. Determination of the kinetics of adsorption

The modeling of batch kinetics helps in explaining the mechanism of adsorption and the potential controlling steps of mass transport. The adsorption behavior of MB in this study best fits the pseudo-second-order kinetic model (Fig. 9). Other models, Elovich, Boyd, liquid film diffusion, and intraparticle diffusion, do not show a good fit.

Among the models tested, pseudo-second-order fits the experimental data better than other kinetic models, indicating the involvement of two species in the sorption process. In agreement with the literature, a pseudo-second-order model best describes the adsorption of divalent ions [29]. The rapid exchange rate, shown to occur in 5 min may mean that exchange positions are, initially at least, on the surface.

3.6. UV-vis spectra investigation

The adsorption of 20 mg/L MB by LC for 40 min results in a change of the blue color of MB to violet. Therefore, to gain insight into the adsorption process, the UV-vis spectrum of MB was subjected to adsorption for 1 h by LC and ATLC. A clear examination of the spectra showed a prominent peak at 560 nm, indicating a shift from the peak of 650 nm. This is an indication that when LC is used for the adsorption of MB, an intermediary product is formed. When ATLC is used, there is a consistent and rapid change in color from blue to colorless during adsorption. It has been reported that the mechanism of the discoloration of MB involves the formation of the reduced form of MB
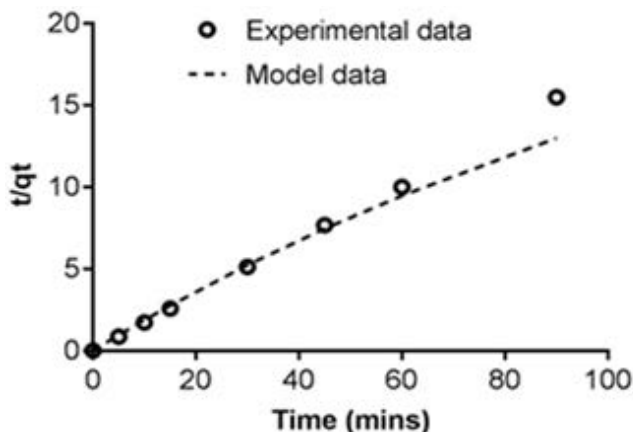
Table 4
Maximum percentage removal of MB ions by other biosorbents

Adsorbent	Initial concentration (g/L)	pH	Time (min)	Percentage removal (%)	Reference
Lignocelluslosic biomatter	10	4	5	>95	[4]
Activated lignin-chitosan	1	7	n/a	87.7	[3]
Modified biochar composites	0.1	12	20	>95	[11]
ATLC (*Luffa cylindrica*)	5	7	5	95.8	This study

Fig. 9. Non-linear regression pseudo-second-order model; (R^2 = 0.997) for MB adsorption at concentration of 20 mg/L, pH 7, and 5 g/L ATLC dosage). Pseudo-second-order model fit is shown by the dashed line.
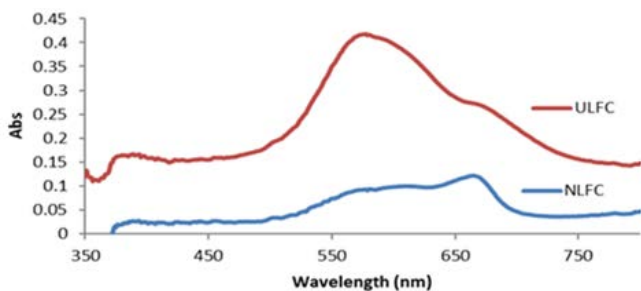

Fig. 10. UV-vis spectra of MB adsorption onto alkali-treated LC (NLFC) and untreated LC (ULFC) at 40 min at pH 7 ± 0.1 at 21°C and 5 g/L alkali-treated and untreated LC dosage); Data from three replicate measurements.

cations (colorless) [41]. This indicates the rapid adsorption of MB without the formation of an intermediary product. This process is initiated by light intensity and indicates the involvement of MB monomer forms for ATLC and the involvement of MB dimer forms for LC [42]. Figs. 10 and 11 present the UV-vis spectra of loofa. The complex formation of methylene blue with untreated loofa and NaOH treated loofa differ over time. This complexation mechanism is explained on the basis of steric hindrance which led to color change. Discoloration of MB (with NaOH treated loofa) is from blue to colorless which involves the formation of the reduced form of MB cations. For untreated loofa, the discoloration occurs from blue to violet and then colorless. This can be explained by chemical variations of MB. Fig. 10 epitomizes that there is an intermediate product that is formed during the adsorption process for untreated loofa at an absorbance at 580 nm wavelength at 40 min [41]. The higher binding constant of NaOH treated loofa indicates the involvement of monomer forms of MB molecules.

Comparing the adsorption of MB under dark and light conditions using HTLC (Fig. 11), there is a difference in MB adsorption in the presence or absence of light. This indicates the effect of light on MB adsorption. A lower MB adsorption capacity (by 2.8%) was found under dark
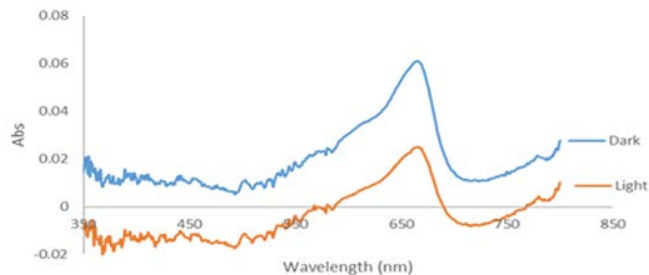

Fig. 11. UV-vis spectra of MB adsorption on acid-treated LC at 5 min under dark and light conditions at pH 7 ± 0.1 at 21°C, 5 g/L HTLC, and 1 h contact time.
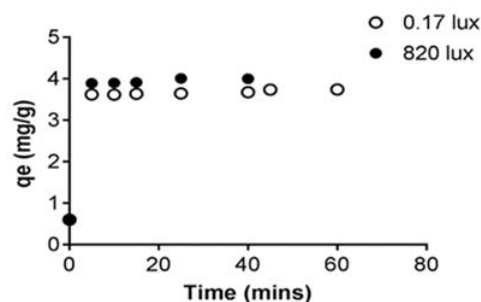

Fig. 12. MB adsorption capacity onto alkali-treated LC at different light intensities overtime at pH 7 ± 0.1, 21°C, 1 h contact time, and 5 g/L alkali-treated LC dosage.

conditions than under light conditions at equilibrium (1 h contact).

3.7. Effect of light intensity on MB adsorption by ATLC

Fig. 12 shows the calculated uptake capacity at a visible light intensity of 0.17 and 820 lux on MB adsorption on alkali-treated loofa (ATLC).

In the presence of light, the overall adsorption capacity of MB onto LC is improved which indicate the involvement of a photodegradative process (Fig. 12). Such photodegradative enhancement of adsorption under different light intensities has also been reported elsewhere [43].

4. Conclusion

The results show that modified loofa is a potentially good biosorbent for the removal of MB (and, by inference, a range of other dyes, and similar compounds) from aqueous solutions. Alkali treatment of loofa enhances the adsorption mechanism by indicating additional free hydroxyl groups. The reactive oxygen species from MB reacts with the free hydroxyl species to form complexes on the loofa surface that optimizes the adsorption of MB. The data show the feasibility of the modified loofa in the removal of MB from aqueous solutions. The FT-IR study indicates the functional groups on the loofa that are involved in MB adsorption. MB uptake efficiency significantly depends on MB ion concentration and pH, but not so much on temperature. The optimum pH of the adsorption was pH 7 at room

temperature (21°C). The removal of MB ions from an aqueous solution is changed by the presence of light. The Freundlich isotherm model predicts the adsorption process better than other models. The pseudo-second-order model is the best-fit to the kinetics. As compared to other recently reported adsorbents, modified loofa has a higher percentage removal, it is economically viable, requires no expensive modification of its properties, utilizes no extensive technological applications for its production, can be acquired in large quantities, and should be regarded as a sustainable adsorption mechanism on a global scale. Loofa could be a good adsorbent.

Acknowledgments

References

[1] J.T. Adeleke, T. Theivasanthi, M. Thiruppathi, M. Swaminathan, T. Akomolafe, A.B. Alabi, Photocatalytic degradation of methylene blue by ZnO/NiFe$_2$O$_4$ nanoparticles, Appl. Surf. Sci., 455 (2018) 195–200.

[2] A. Joseph, K. Vellayan, B. González, M.A. Vicente, A. Gil, Effective degradation of methylene blue in aqueous solution using Pd-supported Cu-doped Ti-pillared montmorillonite catalyst, Appl Clay Sci., 168 (2019) 7–10.

[3] A.B. Albadarin, M.N. Collins, M. Naushad, S. Shirazian, G. Walker, C. Mangwandi, Activated lignin-chitosan extruded blends for efficient adsorption of methylene blue, Chem. Eng. J., 307 (2017) 264–272.

[4] S. Manna, D. Roy, P. Saha, D. Gopakumar, S. Thomas, Rapid methylene blue adsorption using modified lignocellulosic materials, Process Saf. Environ. Prot., 107 (2017) 346–356.

[5] U.G. Akpan, B.H. Hameed, Photocatalytic degradation of wastewater containing acid red 1 by titanum oxide: effect of calcination temperature, Desal. Water Treat., 43 (2012) 84–90.

[6] S.R. Patil, U.G. Akpan, B.H. Hameed, S.K. Samdarshi, A comparative study of photocatalytic efficiency of Degussa P25 Qualigens and Humbikat UV-100 in the degradation kinetic of Congo red dye, Desal. Water Treat., 46 (2012) 188–195.

[7] U.G. Akpan, B.H. Hameed, Solar degradation of an azo dye, acid red 1, by Ca–Ce–W–TiO$_2$ composite catalyst, Chem. Eng. J., 169 (2011) 91–99.

[8] X. Liu, D.J. Lee, Thermodynamic parameters for adsorption equilibrium of heavy metals and dyes from wastewaters, Bioresour. Technol., 160 (2014) 24–31.

[9] M.K. Dahri, M.R.R. Kooh, L.B.L. Lim, Application of *Casuarina equisetifolia* needle for the removal of methylene blue and malachite green dyes from aqueous solution, Alexandria Eng. J., 54 (2015) 1253–1263.

[10] I. Tsibranska, E. Hristova, Comparison of different kinetic models for adsorption of heavy metals onto activated carbon from apricot stones, Bulg. Chem. Commun., 43 (2011) 370–377.

[11] M. Ajuru, F. Nmom, A review on the economic uses of species of *Cucurbitaceae* and their sustainability in Nigeria, Am. J. Plant. Biol., 2 (2017) 17–24.

[12] L.A. Agbabiaka, K.C. Okorie, C.F. Ezeafulukwe, Plantain peels as dietary supplement in practical diets for African catfish (*Clarias gariepinus* burchell 1822) fingerlings, Agric. Biol. J. North Am., 4 (2013) 155–159.

[13] A. Emene, R. Edyvean, Removal of Pb(II) ions from solution using chemically modified *Luffa cylindrica* as a method of sustainable water treatment, Int. J. Sci. Eng. Res., 10 (2019) 344–364.

[14] S. Banerjee, M.C. Chattopadhyaya, Adsorption characteristics for the removal of a toxic dye, tartrazine from aqueous solutions by a low cost agricultural by-product, Arabian J. Chem., 10 (2013) S1629–S1638, doi: 10.1016/j.arabjc.2013.06.005.

[15] B. Ozkaya, Adsorption and desorption of phenol on activated carbon and a comparison of isotherm models, J. Hazard. Mater., 129 (2006) 158–163.

[16] X. Chen, Modeling of experimental adsorption isotherm data, Information, 6 (2015) 14–22.

[17] K.Y. Foo, B.H. Hameed, Insights into the modeling of adsorption isotherm systems, Chem. Eng. J., 156 (2010) 2–10.

[18] M. Arshadi, M. Mehravar, M.J. Amiri, A.R. Faraji, Synthesis and adsorption characteristics of an heterogenized manganese nanoadsorbent towards methyl orange, J. Colloid Interface Sci., 440 (2015)189–197.

[19] B. Yang, J. Zuo, J.X.X. Tang, F. Liu, X. Yu, X.X. Tang, Effective ultrasound electrochemical degradation of methylene blue wastewater using a nanocoated electrode, Ultrason. Sonochem., 21 (2014) 1310–1317.

[20] G. Nong, Z. Zhou, S. Wang, Generation of hydrogen, lignin and sodium hydroxide from pulping black liquor by electrolysis, Energies, 9 (2015) 13, doi: 10.3390/en9010013.

[21] L. Ghali, S. Msahli, M. Zidi, F. Sakli, Effect of pre-treatment of Luffa fibres on the structural properties, Mater. Lett., 63 (2009) 61–63.

[22] N. Fathy, O.I. El-Shafey, L.B. Khalil, Effectiveness of alkali-acid treatment in enhancement the adsorption capacity for rice straw: the removal of methylene blue dye, Phys. Chem., 2013 (2013) 1–15.

[23] D. Williams, I. Fleming, Spectroscopic Methods in Organic Chemistry, Thieme, Stuttgart, 2008.

[24] P. Saueprasearsit, M. Nuanjaraen, M. Chinlapa, Biosorption of lead (Pb^{2+}) by *Luffa cylindrica* fiber, Enviorn. Res. J., 4 (2010) 157–166.

[25] B.T. Ngwenya, J. Tourney, M. Magennis, L. Kapetas, V. Olive, A surface complexation framework for predicting water purification though metal biosorption, Desalination, 248 (2009) 344–351.

[26] J.J. Salazar-rabago, R. Leyva-ramos, J. Rivera-utrilla, R. Ocampo-Perez, F.J. Cerino-Cordova, Biosorption mechanism of Methylene Blue from aqueous solution onto White Pine (*Pinus durangensis*) sawdust: effect of operating conditions, Sustainable Environ. Res., 27 (2017) 32–40.

[27] X. Li, D. Liao, X. Xu, Q. Yang, G. Zeng, W. Zheng, Kinetic studies for the biosorption of lead and copper ions by *Penicillium simplicissimum* immobilized within loofa sponge, J. Hazard. Mater., 159 (2008) 610–615.

[28] N. Boudechiche, H. Mokaddem, Z. Sadaoui, M. Trari, Biosorption of cationic dye from aqueous solutions onto lignocellulosic biomass (*Luffa cylindrica*): characterization, equilibrium, kinetic and thermodynamic studies, Int. J. Ind. Chem., 7 (2016) 167–180.

[29] V.J.P. Vilar, C.M.S. Botelho, J.P.S. Pinheiro, R.F. Domingos, R.A.R. Boaventura, Copper removal by algal biomass: biosorbents characterization and equilibrium modelling, J. Hazard. Mater., 163 (2009) 1113–1122.

[30] M. Peydayesh, A. Rahbar-Kelishami, Adsorption of methylene blue onto *Platanus orientalis* leaf powder: kinetic, equilibrium and thermodynamic studies, J. Ind. Eng. Chem., 21 (2015) 1014–1019.

[31] X. Tang, Y. Li, R. Chen, F. Min, J. Yang, Y. Dong, Evaluation and modeling of methyl green adsorption from aqueous solutions using loofah fibers, Korean J. Chem. Eng., 32 (2014) 125–131.

[32] X.-K. OuYang, L.-P. Yang, Z.-S. Wen, Adsorption of Pb(II) from solution using peanut shell as biosorbent in the presence of amino acid and sodium chloride, Bioresources, 9 (2014) 2446–2458.

[33] C. Liu, C. Yan, S. Zhou, W. Ge, Fabrication of sponge biomass adsorbent through UV-induced surface-initiated polymerization for the adsorption of Ce(II) from wastewater, Water Sci. Technol., 75 (2017) 2755–2764.

[34] H.N. Bhatti, A. Jabeen, M. Iqbal, S. Noreen, Z. Naseem, Adsorptive behavior of rice bran-based composites for

malachite green dye: isotherm, kinetic and thermodynamic studies, J. Mol. Liq., 237 (2017) 322–333.

[35] M.R. Sangi, A. Shahmoradi, J. Zolgharnein, G.H. Azimi, M. Ghorbandoost, Removal and recovery of heavy metals from aqueous solution using Ulmus carpinifolia and Fraxinus excelsior tree leaves, J. Hazard. Mater., 155 (2008) 513–522.

[36] N. Feng, X. Guo, S. Liang, Y. Zhu, J. Liu, Biosorption of heavy metals from aqueous solutions by chemically modified orange peel, J. Hazard. Mater., 185 (2011) 49–54.

[37] R. Ahmad, S. Haseeb, Kinetic, isotherm and thermodynamic studies for the removal of Pb^{2+} ion by a novel adsorbent *Luffa acutangula* (LAPR), Desal. Water Treat., 57 (2015) 17826–17835.

[38] H. Benhima, M. Chiban, F. Sinan, P. Seta, M. Persin, Removal of lead and cadmium ions from aqueous solution by adsorption onto micro-particles of dry plants, Colloids Surf., B, 61 (2008) 10–16.

[39] I. Oboh, E. Aluyor, T. Audu, Biosorption of heavy metal ions from aqueous solutions using a biomaterial, Leonardo J. Sci., 14 (2009) 58–65.

[40] T.A. Khan, E.A. Khan, Shahjahan, Adsorptive uptake of basic dyes from aqueous solution by novel brown linseed deoiled cake activated carbon: equilibrium isotherms and dynamics, J. Environ. Chem. Eng., 4 (2016) 3084–3095.

[41] M.A. Tabbara, M.M. El Jamal, A kinetic study of the discoloration of methylene blue by Na_2SO_3, comparison with NaOH, J. Univ. Chem. Technol. Metall., 47 (2012) 275–282.

[42] B. Samiey, F. Ashoori, Adsorptive removal of methylene blue by agar: effects of NaCl and ethanol, Chem. Cent. J., 1 (2012) 1–13.

[43] N. Soltani, E. Saion, M.Z. Hussein, M. Erfani, A. Abedini, Visible light-induced degradation of methylene blue in the presence of photocatalytic ZnS and CdS nanoparticles, Int. J. Mol. Sci., 4 (2012) 12242–12258.
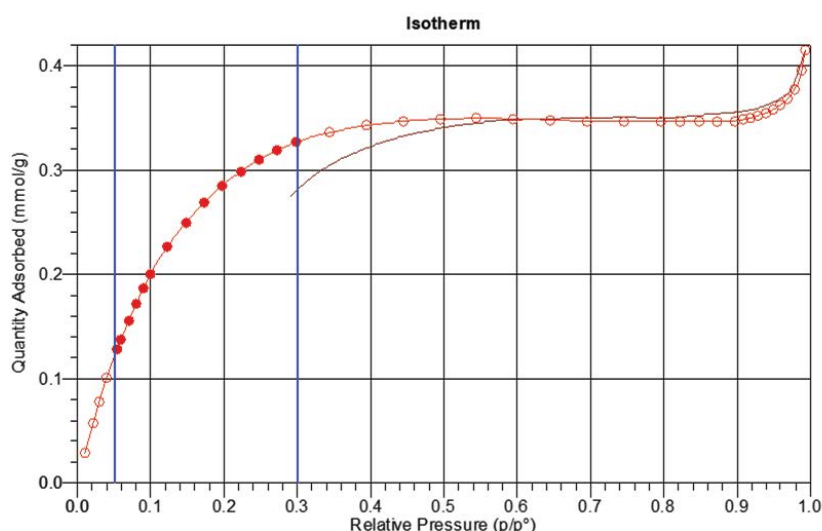
Supplementry Information

Fig. S1. Adsorption isotherm of HCl treated loofa showing the quantity absorbed onto the pores vs. the relative pressure (monolayer complete adsorption between 0.05 and 0.3).